TU Delft

Delft University of Technology

Algorithm to suppress drift for micro-mirror and other intensity modulated hydrogen sensors

Bannenberg, Lars J.

DOI
10.1109/JSEN.2023.3328642

Publication date
2023

Document Version
Final published version

Published in
IEEE Sensors Journal

Citation (APA)
Bannenberg, L. J. (2023). Algorithm to suppress drift for micro-mirror and other intensity modulated hydrogen sensors. *IEEE Sensors Journal*, *23*(24), 30720-30727. https://doi.org/10.1109/JSEN.2023.3328642

Important note
To cite this publication, please use the final published version (if applicable).
Please check the document version above.

Copyright
Other than for strictly personal use, it is not permitted to download, forward or distribute the text or part of it, without the consent of the author(s) and/or copyright holder(s), unless the work is under an open content license such as Creative Commons.

Takedown policy
Please contact us and provide details if you believe this document breaches copyrights.
We will remove access to the work immediately and investigate your claim.

This work is downloaded from Delft University of Technology.
For technical reasons the number of authors shown on this cover page is limited to a maximum of 10.

Algorithm to Suppress Drift for Micromirror and Other Intensity-Modulated Hydrogen Sensors

Lars J. Bannenberg

***Abstract*—Here, a method to suppress drift in intensity-modulated sensors is presented that preserves the advantages of such sensors including simplicity and low-cost components. This method is illustrated using metal hydride-based optical hydrogen sensors that can reliably, accurately, and quickly sense hydrogen across a large concentration range. These sensors rely on a metal hydride-sensing material that reversibly absorbs hydrogen when a hydrogen concentration is present. In turn, this causes a change in the optical properties which can be probed to determine the hydrogen concentration. To do this, two major methods exist: intensity- and frequency-modulated sensors. While intensity-modulated sensors are typically simpler and cheaper to fabricate, they may suffer from drifting light sources and unstable alignments. Using the fact that exposure to hydrogen reduces (increases) the optical transmission (reflectivity) of a Ta-based sensing material for blue/green light while it increases (decreases) the transmission for (near) infrared (IR) light, it is possible to differentiate between a changing hydrogen concentration and a drifting light source: Whereas the signal of both wavelengths is positively correlated for a drifting light source, the signal is negatively correlated when the hydrogen concentration changes. Using this algorithm, the drift on the signal can be reduced by a factor of 5 for intensity-modulated sensors. In a more general perspective, the wealth of information in the wavelength-dependent optical response allows for more advanced approaches to improve the signal and accuracy of (optical) sensors.**

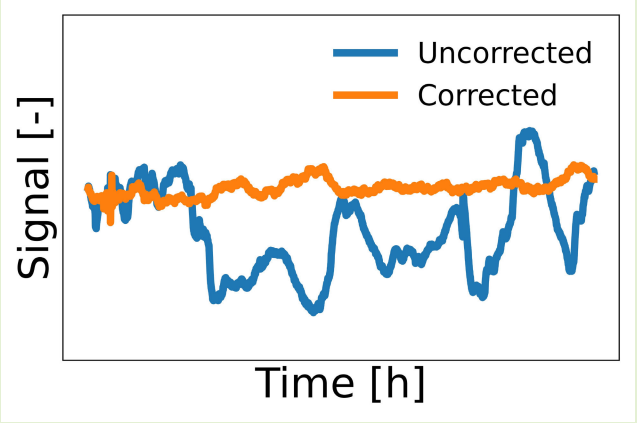

***Index Terms*— Algorithm, drift, optical hydrogen sensing.**

I. Introduction

HYDROGEN is envisioned to play a major role in the transition to a green economy, both as a large-scale storage medium and as a feedstock for the chemical industry [1], [2], [3], [4]. As hydrogen–air mixtures can be flammable or even explosive, accurate and reliable hydrogen sensors that can detect the smallest concentration of hydrogen leakages are pivotal for the safe and successful implementation of hydrogen as an energy carrier. Such leakages are also important to detect from an environmental point of view as hydrogen is an indirect greenhouse gas, and hydrogen sensors may also be used for performance monitoring and enhancement of devices such as fuel cells [5], [6], [7].

Optical metal hydride hydrogen sensors feature major benefits over other types of sensors such as their large sensing range, fast response, and the fact that they are inherently safe: no currents are required near the sensing area [8], [9], [10], [11], [12], [13], [14]. These optical sensors rely on a metal hydride-sensing material that gradually and reversibly absorbs hydrogen when hydrogen is present in the vicinity of the sensor. In turn, the absorbed hydrogen changes the optical properties of the metal hydride, which can then be probed to determine the hydrogen concentration/pressure. To do this, two major methods can be distinguished: intensity- and frequency-modulated hydrogen sensors. In intensity-modulated sensors, the optical transmission or reflectivity of the sensing material is probed, such as in a micromirror sensor [15], [16], [17]. In frequency-modulated sensors, such as fiber-Bragg gratings [18], [19], [20] and (localized) surface plasmon resonance sensors [9], [12], [21], [22], [23], the exposure of the sensor to hydrogen causes a wavelength shift. While frequency-modulated sensors have the substantial advantage that they are not sensitive to intensity fluctuations of the light sources and are therefore more stable than intensity-modulated sensors, they contain more complex and expensive components. In particular, the drifting intensity of the light source or detection efficiency compromises

Manuscript received 20 October 2023; accepted 27 October 2023. Date of publication 9 November 2023; date of current version 14 December 2023. The associate editor coordinating the review of this article and approving it for publication was Dr. Xuehao Hu.

The author is with the Faculty of Applied Sciences, Delft University of Technology, 2629 Delft, The Netherlands (e-mail: l.j.bannenberg@tudelft.nl).

Digital Object Identifier 10.1109/JSEN.2023.3328642

1558-1748 © 2023 IEEE. Personal use is permitted, but republication/redistribution requires IEEE permission.
See https://www.ieee.org/publications/rights/index.html for more information.

Authorized licensed use limited to: TU Delft Library. Downloaded on January 18,2024 at 13:07:31 UTC from IEEE Xplore. Restrictions apply.

the accuracy and long-term stability of intensity-modulated sensors.

Here, the fact that Pd-alloy-capped tantalum-based hydrogen-sensing materials [24], [25], [26], [27] feature an opposite optical response to hydrogen for green/blue and infrared (IR) light is used to effectively suppress drift due to, for example, the fluctuations of the light source using a simple algorithm. While in this case, Ta-based alloys are primarily selected as the direction of the optical response to changing hydrogen concentrations is different for different wavelengths, these materials offer good hydrogen-sensing properties in terms of the magnitude of the optical contrast, absence of hysteresis, response time, and concentration range that can be probed. Indeed, while the optical transmission (reflectivity) increases (decreases) upon exposure to hydrogen for blue and green light, it decreases (increases) for (near) IR light when the material is exposed to hydrogen. The algorithm uses this property and is based on the idea that fluctuations of the light source cause the same response to both the green/blue and IR light signal, that is, they are positively correlated. Differently, a change in hydrogen causes an opposite response to the detected green and IR light response, that is, these signals are negatively correlated. Using this approach, the drift can substantially be suppressed ensuring an accurate determination of the hydrogen concentration. As a side gain, this simple algorithm can also increase the resolution of the hydrogen sensor. As such, the algorithm in combination with a sensing stack with the property of opposite responses to hydrogen for different wavelengths, substantially enhances the performance of intensity-modulated hydrogen sensors while preserving the simplicity and cost advantages of an intensity-modulated sensor.

II. Experimental

The thin-film sample, consisting of a 4-nm Ti adhesion layer, a 20-nm $Ta_{0.88}Pd_{0.12}$ sensing layer, and a 30-nm $Pd_{0.6}Au_{0.4}$ capping layer to catalyze the hydrogen dissociation and recombination reaction and prevent the film from oxidation (nominal thicknesses), was deposited on 10 × 10 mm^2 quartz substrates with a thickness of 0.5 mm and surface roughness <0.4 nm (Mateck GmbH, Jülich, Germany) using magnetron sputtering. The deposition was performed in 0.3 Pa of Ar by magnetron sputtering in an ultrahigh vacuum chamber (AJA Int.) with a base pressure of 10^{-6} Pa. During deposition, the substrates were rotated to enhance the homogeneity. The deposition rates of the layers were 0.10 nm s^{-1} (125 W dc) for Ta, 0.05 nm s^{-1} (100 W dc) for Ti, 0.13 nm s^{-1} (50 W dc) for Pd, and 0.11 nm s^{-1} (25 W dc) for Au. All targets have a diameter of 5.08 mm (2 in) and a purity of at least 99.9% (Mateck GmbH, Jülich, Germany). Before the deposition, the Ta target was presputtered for 10 min to avoid possible contamination from the tantalum oxide and nitride layers present at the surface of the target.

The sample was checked for layer thickness and quality with X-ray reflectometry (XRR) and X-ray diffraction (XRD) using a Bruker D8 Discover (Cu-Kα $\lambda = 0.1542$ nm) equipped with a LYNXEYE XE detector (Bruker AXS GmbH, Karlsruhe, Germany). XRD measurements were performed with a Göbel mirror and a 0.6-mm fixed slit on the primary and two 0.6-mm slits on the secondary side with the detector operated in the 0-D mode. These measurements revealed that $Pd_{0.6}Au_{0.4}$ is textured with the ⟨111⟩ direction out-of-plane and that $Ta_{0.88}Pd_{0.12}$ crystallized in the body-centered cubic α-Ta phase with ⟨110⟩ out-of-plane. Differently, for the XRR measurements, three 0.1-mm slits were used. The data were fit with GenX3 [28], [29] to obtain estimates for the layer thickness, roughness, and density of the thin films. The fits show that the thickness of $Pd_{0.6}Au_{0.4}$ is 30.0 nm with a root-mean-square roughness of 1 nm and a thickness of 19.5 nm and roughness of 1 nm for $Ta_{0.88}Pd_{0.12}$.

The optical measurements under various hydrogen concentrations/pressures were performed in a flow setup. The setup consists of a small custom-made pressure cell with quartz windows to allow optical transmission. For the transmission measurements, one fiber is placed below and one above the cell. For the reflection measurements, two fibers are mounted under 30°. In both cases, one fiber transports the light from the Ocean Optics HL-2000-FSHA halogen light source (Ocean Insights Orlando, FL, USA). The intensity of the light from the fiber can be adjusted with a Thorlabs Cage System Iris Diaphragm with a diameter of 0.8–20 mm (Thorlabs, Inc., Newton, New Jersey, USA), after which it is focused on the sample with lenses. The reflected or transmitted light is coupled into the other optical fiber connected to an Ocean Optics Maya2000 Pro Series Spectrometer (Ocean Insights, Orlando, FL, USA). During processing, the output from the spectrometer was corrected by subtracting the background signal of the spectrometer deduced by measuring with the shutter closed ("dark" measurement).

To set the flow and hydrogen concentration, three flow controllers were used with a flow of 0–100 s.c.c.m., 0–200 s.c.c.m., and 0–250 s.c.c.m. (Thermal Mass GF Series, Brooks Instrument, Hatfield, PA, USA). One of these flow controllers is connected to the Ar gas network (5 N purity), whereas the other two to either gas mixtures of 0.1% H_2 and 4% H_2 in Ar and 100% H_2 ($\Delta c_{H2}/c_{H2} < 2\%$, Linde Gas Benelux BV, Dieren, The Netherlands). The setup is located inside a lab in which the temperature is 19.5 °C and fluctuates by ±0.5 °C.

III. Results

The idea of the algorithm that is illustrated in Fig. 1 is that it can discriminate between a change in hydrogen concentration and a fluctuation of the light source by considering the optical response of two wavelengths of light: one of which is the transmission/reflection increases monotonically with increasing hydrogen concentration, and one of which the transmission/reflection decreases monotonically with increasing hydrogen concentration. If this is the case, then the response of the two wavelengths is positively correlated in the case of fluctuations in the light source, while they are negatively correlated when the hydrogen concentration/pressure is changing.

To realize such a sensor, a sensing material stack is needed that has the properties of: 1) opposite response to changing hydrogen concentration for different wavelengths; 2) that this

Authorized licensed use limited to: TU Delft Library. Downloaded on January 18,2024 at 13:07:31 UTC from IEEE Xplore. Restrictions apply.

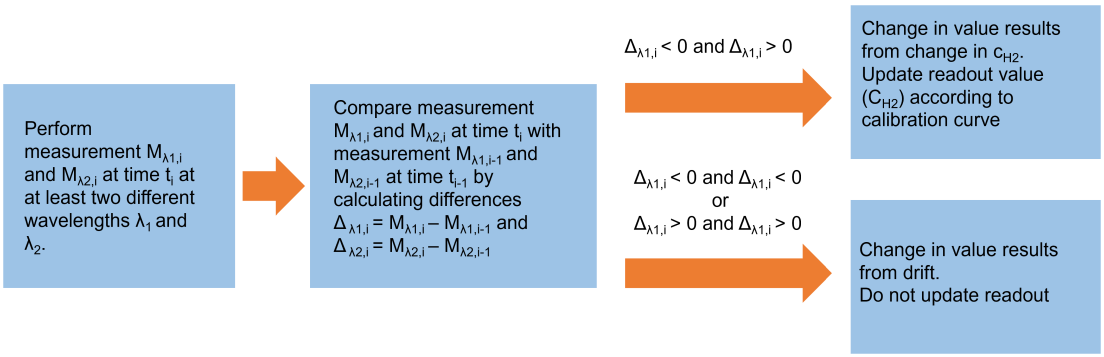

Fig. 1. Flowchart describing how the algorithm suppresses drift. For the method to work optimally, the two signals M_{λ_1} and M_{λ_2} should be positively correlated when the hydrogen concentration stays constant and negatively correlated when the hydrogen concentration changes.

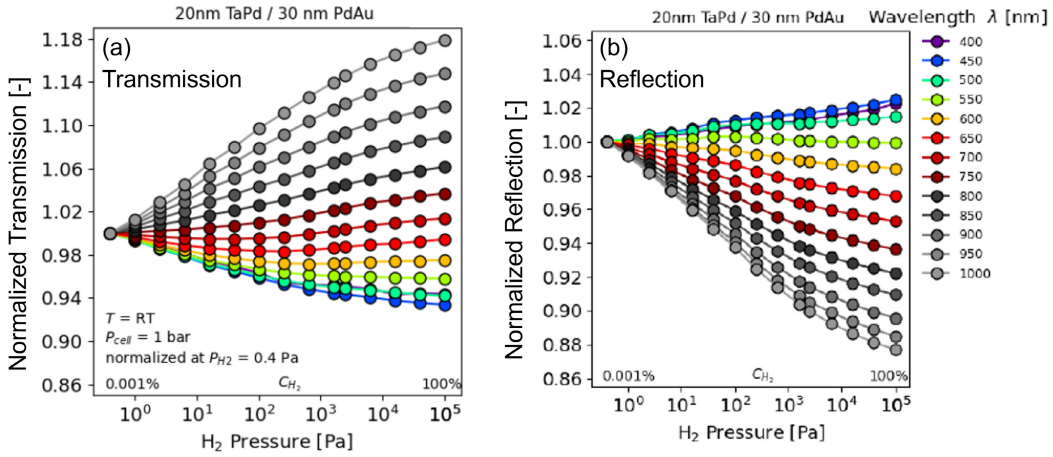

Fig. 2. Wavelength-dependent optical (a) transmission and (b) reflectivity of a thin film with a 4-nm Ti adhesion layer, a 20-nm $Ta_{0.88}Pd_{0.12}$ sensing layer, and a 30-nm $Pd_{0.6}Au_{0.4}$ capping layer when exposed stepwise to various concentrations of hydrogen in an Ar atmosphere at a constant pressure of 1 bar. The data are normalized to the optical transmission/reflectivity at $c_{H2} = 0.001\%$ / $P_{H2} = 1$ Pa. Data adapted from [31].

change is monotonous; and 3) the optical response is free of hysteresis. Tantalum-alloy materials such as $Ta_{1-y}Pd_y$ fulfill all these requirements [24], [25], [26], [27], together with a sensing response of at least seven orders of magnitude both at room and elevated temperatures. Such materials are typically combined with a capping layer that catalyzes the hydrogen dissociation reaction and protects the sensing layer from, for example, oxidation [30].

Fig. 2 shows that such an opposite response to hydrogen can indeed be realized for a $Ta_{0.88}Pd_{0.12}$ sensing layer, both in transmission and reflection. For a thin film with a 4-nm Ti adhesion layer, a 20-nm $Ta_{0.88}Pd_{0.12}$ sensing layer and a 30-nm $Pd_{0.6}Au_{0.4}$ capping layer, the film was exposed to different hydrogen concentrations in argon using a flow setup while measuring the optical transmission and reflection (under 30°) with a halogen light source and spectrometer at room temperature. Fig. 2 illustrates that the optical transmission decreases monotonously for blue and green light ($\lambda = 450$, 500 nm) with increasing hydrogen concentration by about 6% between $c_{H2} = 0.001\%$ and 100%. Differently, the optical transmission increases monotonically for near-IR light by up to 18% between $c_{H2} = 0.001\%$ and 100%. Similar responses, yet in opposite directions, are found for reflection.

The next prerequisite for such an algorithm to work is that the drift in signal between the different wavelengths is positively correlated. To test this, the optical transmission of a thin film was monitored for about a week at a constant hydrogen concentration. Fig. 3(a) shows that indeed a drift is visible in the signal, including some spikes. Over this week's time, a maximum change in transmission of about 0.4% was observed. Especially for the green light, this is about 10% of the entire signal change when the hydrogen concentration is increased from 0.001% to 100% and would thus result in a substantial measurement error. This highlights that the large effect drift can have on the sensor's reading.

Most importantly, Fig. 3(a) shows that the signal of the different wavelengths is strongly correlated, following the same spikes in the data. Indeed, the correlation between the various green/blue light wavelengths, on the one hand, and the IR light varies between 0.9 and 0.98, being the largest between $\lambda =$ 535 and 895 nm light.

As a first step, an algorithm is considered that averages every 150 s the optical response and then checks whether the change in the optical response of both the $\lambda = 535$ and 895 nm channel is positive or negative. If both changes are positive or negative, then the algorithm identifies this as drift and does not update the reading. If the two signals show a positive and

Authorized licensed use limited to: TU Delft Library. Downloaded on January 18,2024 at 13:07:31 UTC from IEEE Xplore. Restrictions apply.

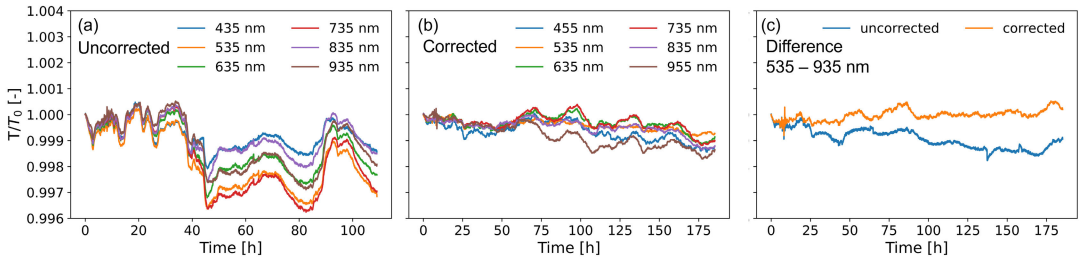

Fig. 3. Wavelength-dependent optical transmission of a thin film with a 4-nm Ti adhesion layer, a 20-nm $Ta_{0.88}Pd_{0.12}$ sensing layer, and a 30-nm $Pd_{0.6}Au_{0.4}$ capping layer was measured for about one week when exposed to a constant hydrogen concentration at room temperature. The data is normalized to the optical transmission/reflectivity at $t = 0$. (a) Uncorrected data. (b) Data corrected with the algorithm. (c) Subtraction of the optical response at λ = 935 nm from the one at $\lambda = 535$ nm.

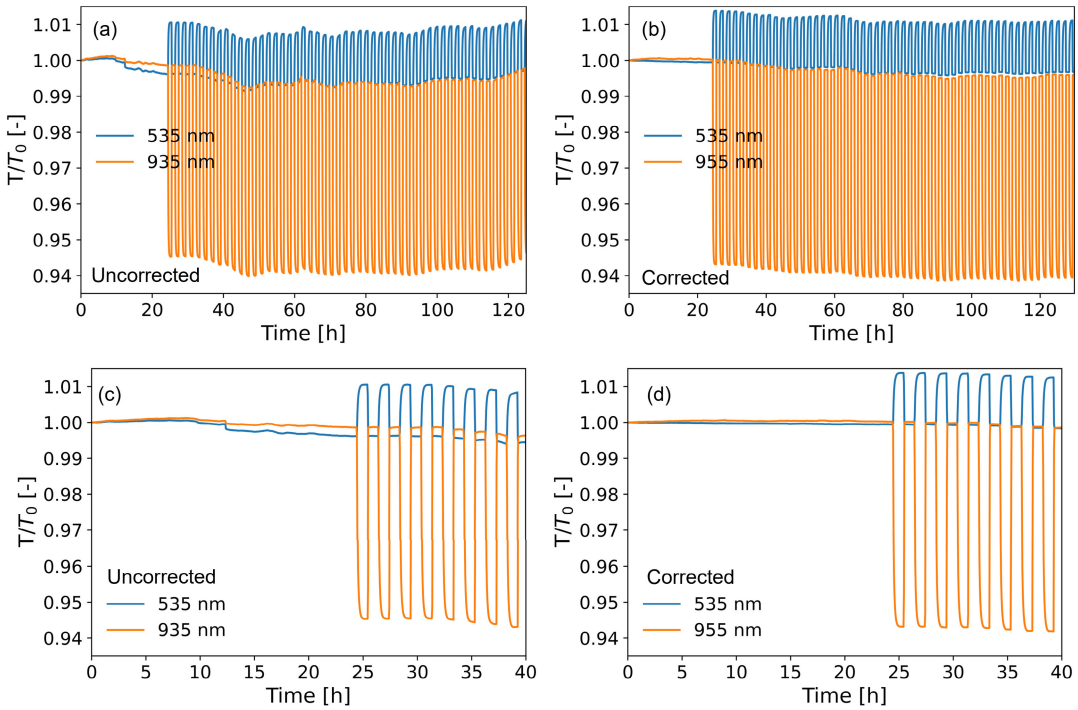

Fig. 4. Wavelength-dependent optical transmission of a thin film with a 4-nm Ti adhesion layer, a 20-nm $Ta_{0.88}Pd_{0.12}$ sensing layer, and a 30-nm $Pd_{0.6}Au_{0.4}$ capping layer measured for about one week when exposed for 24 h to $c_{H2} = 4\%$ and then alternatively for 1 h to $c_{H2} = 4\%$ followed by 1 h to c_{H2} = 0.005%. The data is normalized to the optical transmission at $t = 0$ h. (a) Uncorrected data. (b) Data corrected with the algorithm. (c) and (d) Closeup of the first 40 h for the uncorrected and corrected data, respectively.

a negative change, or vice versa, then the algorithm considers it as a change in hydrogen concentration and updates the response. It is important that the time period (or periods) should be chosen long enough to ensure that the changes in the signal are not dominated by noise. Furthermore, it is noted that a rolling window algorithm can be implemented to provide a live update of the signal or more advanced approaches where instead of a fixed time period a fixed step size in the transmission is taken (e.g., step of 2× the noise level) or more wavelength ranges are used.

Fig. 3(b) shows the corrected response by this algorithm and illustrates that the algorithm can suppress the drift of the signal by up to a factor of 5.6. This is further detailed in Tables I and II that report that for, for example, $\lambda = 535$ nm light, the algorithm reduces the maximum deviation from 0.39% to 0.07%, that is, an improvement by a factor of 5.6. In the remainder of the article, drift is referred to as the maximum change of the signal keeping all other parameters different during a specified time period.

Another simple approach would be to simply subtract the response at $\lambda = 935$ nm from the one at $\lambda = 535$ nm. Fig. 3(c) shows the result: compared to the individual responses, the absolute drift is reduced, by up to a factor of 1.5 using this "difference method."

To see how both responses are affected when hydrogen pressures are changed or when the signal is distorted deliberately by moving the optical fibers connected to both the light source and the spectrometer, a new measurement was performed. First, the sample was left for 24 h at $c_{H2} = 4\%$, while at $t = 12$ h, the optical fibers were moved. Subsequently, from $t = 24$ h onward, the sample was alternatively exposed for 1 h to $c_{H2} = 4\%$ followed by 1 h at $c_{H2} = 0.005\%$,

Authorized licensed use limited to: TU Delft Library. Downloaded on January 18,2024 at 13:07:31 UTC from IEEE Xplore. Restrictions apply.

TABLE I

STANDARD DEVIATION (STD. DEV.) AND MAXIMUM DEVIATION FROM ONE OF THE WAVELENGTH-DEPENDENT OPTICAL TRANSMISSION NORMALIZED TO THE OPTICAL TRANSMISSION AT $t = 0$ OF A THIN FILM WITH A 4-NM TI ADHESION LAYER, A 20-NM $Ta_{0.88}Pd_{0.12}$ SENSING LAYER, AND A 30-NM $Pd_{0.6}Au_{0.4}$ CAPPING LAYER MEASURED FOR ABOUT ONE WEEK WHEN EXPOSED TO A CONSTANT HYDROGEN CONCENTRATION AT ROOM TEMPERATURE, THAT IS, THE DATA OF FIG. 3. $T_{4\%}/T_{0.005\%}$ REFERS TO THE TRANSMISSION OF THE FILM AT c_{H2} = 4% DIVIDED BY THE TRANSMISSION AT $c_{H2} = 0.005\%$. ALL METRICS ARE REPORTED FOR BOTH THE UNCORRECTED AND DATA CORRECTED WITH THE ALGORITHM. 530–930 NM REFERS TO THE SIGNAL OBTAINED WHEN THE SIGNAL OF λ = 935 NM IS SUBTRACTED FROM THE ONE AT $\lambda = 535$ NM ("DIFFERENCE METHOD")

λ [nm]	std. dev.		maximum		$T_{4\%}/T_{0.005\%}$
	Uncorrected	Corrected	Uncorrected	Corrected	
435	0.0005	0.0003	0.0021	0.0011	1.0108
535	0.0011	0.0003	0.0039	0.0007	1.0150
635	0.0010	0.0003	0.0032	0.0009	1.0090
735	0.0013	0.0003	0.0038	0.0008	0.9850
835	0.0008	0.0002	0.0026	0.0008	0.9670
935	0.0010	0.0004	0.0029	0.0012	0.9460
535-935	0.0004	0.0002	0.0018	0.0008	1.0690

TABLE II

DRIFT REDUCTION BY THE ALGORITHM BASED ON THE METRICS OF TABLE I AS WELL AS THE DRIFT RELATIVE TO THE AMPLITUDE OF THE NORMALIZED CHANGE IN TRANSMISSION OF THE FILM WHEN THE HYDROGEN PRESSURE IS CHANGED FROM $c_{H2} = 0.005\%$ DIVIDED BY THE TRANSMISSION AT $c_{H2} = 4.0\%$. THESE METRICS ARE REPORTED FOR BOTH THE UNCORRECTED AND DATA CORRECTED WITH THE ALGORITHM. 530–930 NM REFERS TO THE SIGNAL OBTAINED WHEN THE SIGNAL OF $\lambda = 935$ NM IS SUBTRACTED FROM THE ONE AT $\lambda = 535$ NM ("DIFFERENCE METHOD")

λ [nm]	drift reduction		std. dev./amplitude		maximum/amplitude	
	std. dev.	maximum	Uncorrected	Corrected	Uncorrected	Corrected
435	1.6	2.0	20	32	5.2	10.2
535	4.1	5.6	14	58	3.9	21.9
635	3.5	3.6	9	33	2.8	10.0
735	3.9	5.0	12	46	4.0	20.0
835	3.6	3.1	39	141	12.7	39.9
935	2.5	2.4	54	133	18.6	43.9
535-935	1.9	2.3	186	345	38.3	86.2

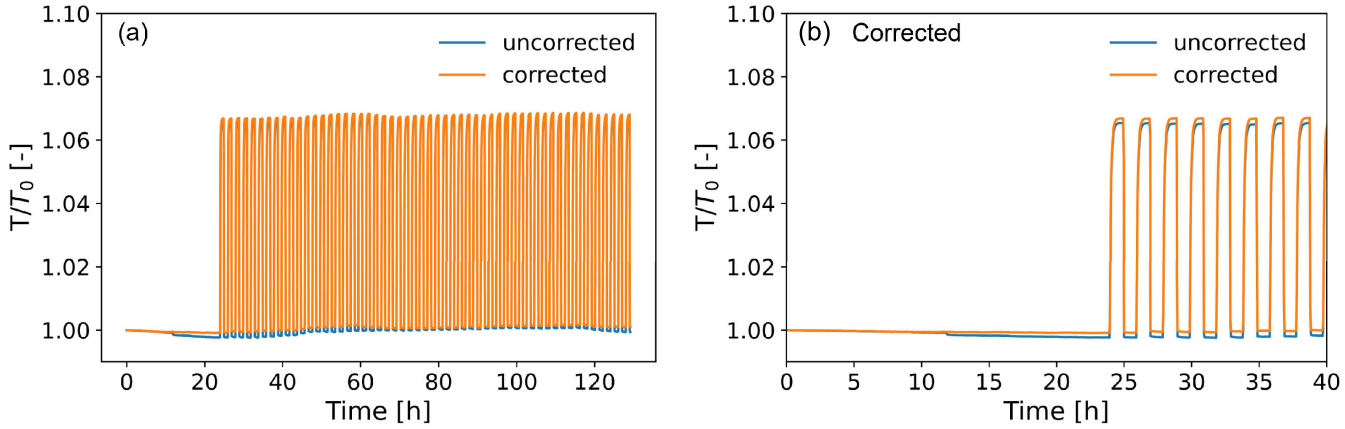

Fig. 5. Optical transmission at $\lambda = 935$ nm subtracted from the one at $\lambda = 535$ nm of a thin film with a 4-nm Ti adhesion layer, a 20-nm $Ta_{0.88}Pd_{0.12}$ sensing layer, and a 30-nm $Pd_{0.6}Au_{0.4}$ capping layer measured for about one week when exposed for 24 h to $c_{H2} = 4\%$, during which at $t = 12$ h, the optical fibers were deliberately moved. Subsequently, from $t = 24$ h onward, the sample was alternatively exposed for 1 h to $c_{H2} = 4\%$ followed by 1 h to $c_{H2} = 0.005\%$. The figure shows the subtracted data ("difference method") without (labeled "uncorrected" in the figure legend) and with a correction using the "correlation method" (labeled "corrected" in the figure legend) for the (a) full time period and (b) closeup of the first 40 h.

a procedure repeated for four days. The corresponding results can be found in Fig. 4 for the correlation-based approach and in Fig. 5 for the approaches based on taking the difference in the signal between two wavelengths.

Fig. 4 shows that the algorithm can minimize the drift, also between the pressure step. In addition, it filters the abrupt movement of the fiber at $t = 12$ h completely, reducing the overall drift from 0.40% to 0.06% for $\lambda = 535$ nm and from 0.15% to 0.05% for $\lambda = 935$ nm. For the subsequent steps that were applied after $t = 24$ h, a reduction is seen in the maximum deviation (lowest–highest value recorded of the $c_{H2} = 4\%$ level) from 0.64% to 0.3% with respect to just considering $\lambda = 535$ nm and from 0.6% to 0.5% when only $\lambda = 935$ nm would be considered. Similar improvements are observed for the $c_{H2} = 0.005\%$ level.

Authorized licensed use limited to: TU Delft Library. Downloaded on January 18,2024 at 13:07:31 UTC from IEEE Xplore. Restrictions apply.

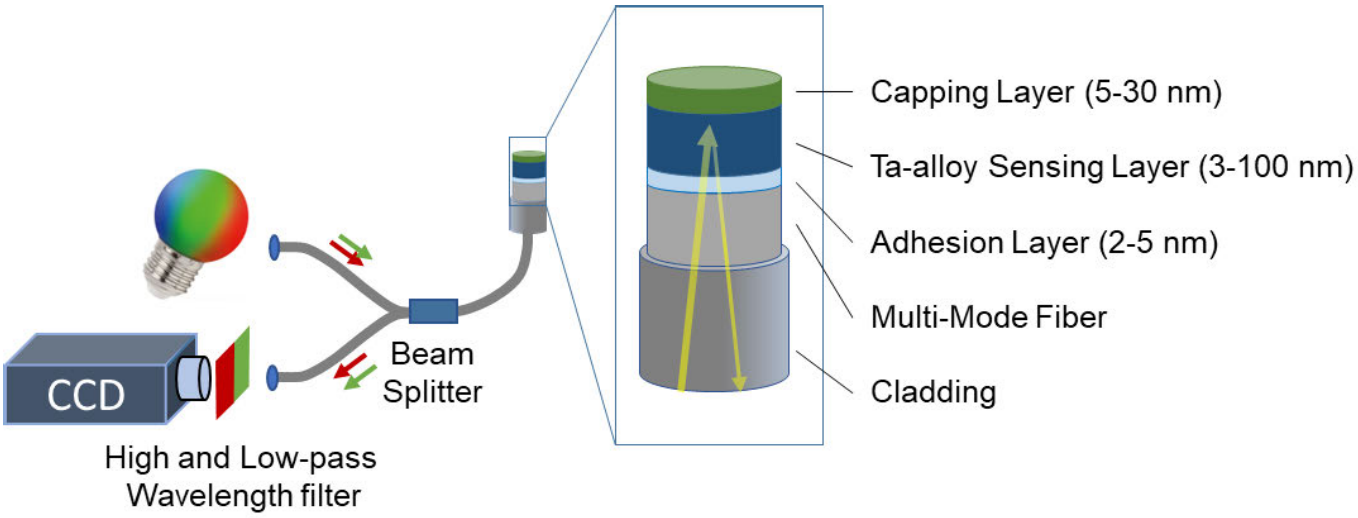

Fig. 6. Schematic representation of a multiwavelength micromirror optical hydrogen sensor. The light, originating from an LED light source that has maxima in both the green and near-IR spectrum, is coupled into the fiber and transported to the tip of the optical fiber sensor. The light is partially reflected by the layer stack deposited on the tip of the fiber (see inset) and then passed back through the fiber and the splitter. The signal is subsequently measured by, for example, a CCD where half of the pixels are covered by a low- and high-pass wavelength filter to measure both the red and green intensities. Upon a change in hydrogen pressure, the hydrogenation of the sensing layer (20–100 nm) changes, which in turn results in a change of the optical properties and thus the amount of light reflected by the layer stack and detected by a photodetector. The sensing layer is cleaved to the substrate by an adhesion layer that is often made of Ti. To prevent oxidation of the sensing layer and to catalyze the hydrogen adsorption, a capping layer (typically a Pd-based alloy) is used. The obtained green and near-IR light signals can be processed digitally or analog to obtain the reading for the hydrogen concentration.

The difference-based algorithm cannot completely remove the change in signal due to the abrupt movement of the fiber at $t = 12$ h as this change is of a different magnitude for the two wavelengths. However, the algorithm does reduce the overall drift substantially by a factor of 2 during the first 24 h. When alternating pressure steps are applied, the difference approach is very effective: it reduces the overall drift during the period $24 < t < 130$ h to 0.28%, that is, by a factor 2.0, significantly more than the factor 1.2 for the correlation-based mechanism at $\lambda = 935$ nm. Indeed, unlike the correlation-based approach, the algorithm can reduce the impact of drift during pressure changes.

The best performance is obtained when both algorithms are combined and the signal obtained with the difference method is corrected with the correlation-based method. In this case, both the drift during a constant hydrogen pressure, the jump in signal when the fibers are moved, and the drift during the alternating pressure steps are reduced substantially. Indeed, in total, this results in the best result and the maximum observed drift over a one-week period (Fig. 3 and Table II) only constitutes 1/86th of the signal when the hydrogen concentration is changed from $c_{H2} = 0.005$ to 4%, significantly better than 1/19th for the best performing individual wavelength. It is noted that a fraction of the remaining drift is due to temperature fluctuations of $\pm$ 0.5 °C. Indeed, the hydrogen-to-metal ratio of the thin film depends not only on the hydrogen concentration in the environment, but also on the temperature around the thin film, and as a result, the optical response is temperature-dependent. Therefore, the reported gains are an understatement. As such, in a real sensor, a temperature sensor needs to be incorporated to translate the change in transmission to a hydrogen concentration.

It is noted that both when using the correlation-based algorithm and when using the difference approach, the observed drift is larger when the hydrogen concentration is changing than when the hydrogen concentration is constant. In the first case, this is likely the result of the fact that during a changing hydrogen pressure, the correlation-based algorithm cannot detect any drift. In the case the difference between the signals is computed, the different magnitude of the response of the two different wavelengths may be at the heart of this. As such, the algorithm is less effective for applications where a change in hydrogen concentration is constantly monitored, such as for hydrogen purity assessments in fuel cells. For safety applications, the algorithm is perfectly suited. In such applications, only incidental changes in the hydrogen concentrations are to be expected.

There are various possibilities to realize a sensor in practice in which these drift-mitigating algorithms are used. Fig. 6 shows one of them based on the micromirror approach where a coating is applied on the tip of a multimode optical fiber. Furthermore, a light source should be used that emits both blue/green and near IR light, such as a green and IR LED or laser powered by the same power supply to ensure that the fluctuations of the light sources are highly correlated. This light is then coupled into the multimode optical fiber. When it reaches the tip of the fiber, it is partially reflected by the metal-hydride coating, and the reflected intensity is subsequently detected by, for example, two photodiodes or a charged coupled device (CCD)/complementary metal oxide semiconductor (CMOS) chip/two diodes of which half of the chip/one diode is covered with an IR light filter (high-pass wavelength filter) and the other half/diode with a green light filter. Subsequently, the signal can be processed both in an analog (simple subtraction) or a digital way. In processing the signal, the temperature of the environment (which should thus be measured separately) should be taken into account to convert the measured signal to a hydrogen concentration. Indeed, the amount of hydrogen

Authorized licensed use limited to: TU Delft Library. Downloaded on January 18,2024 at 13:07:31 UTC from IEEE Xplore. Restrictions apply.

absorbed by a metal hydride-sensing material depends, at a given hydrogen concentration, on temperature, and thus the optical response, and depending on temperature, a different calibration curve should be used (see [10], [32], and [33]).

Furthermore, in realizing such a micromirror sensor, coupling the efficiency of different wavelengths with the same optical coupler is important to avoid high loss of intensity leading to a deterioration of the signal. It is noted that rather than choosing green and IR light, other wavelengths can also be used as long as the change in transmission/reflection of these two wavelengths when a hydrogen concentration is applied is opposite. Additionally, we note that a multimode fiber needs to be used in this case as opposed to when a single wavelength sensor is constructed for which a single-mode fiber is sufficient. A downside of this is that it limits the bending radius of the optical fiber owing to the larger core of the fiber.

IV. Conclusion

In conclusion, this work demonstrates that an opposite response of different wavelengths to a change in hydrogen concentration can be used effectively to enhance the sensing performance and, in particular, reduce drift. Indeed, the fact that the optical transmission (reflectivity) of a palladium-alloy-capped Ta-based sensing material is reduced (increased) for blue/green light when it is exposed to hydrogen while in the same case, the transmission increases or reflectivity decreases for (near) IR light can be used to differentiate between a changing hydrogen concentration and a drifting lamp: Whereas the blue/green and IR signals of a drifting light source are positively correlated, a change in hydrogen concentration causes two negatively correlated signals. While the presented method is simple in nature, it is effective as it can reduce the drift on the signal by a factor of 5. Moreover, the wavelength-dependent optical response allows for more advanced approaches to further improve the signal including incorporating temperature effects and using artificial intelligence as well as applications beyond the field of hydrogen sensing.

Acknowledgment

Herman Schreuders is thanked for preparing the sample. Kasun Dissanayake is thanked for proofreading the manuscript. Bart Boshuizen is acknowledged for designing and maintaining the Labview software to control the pressure cells. Erwin Janssen is thanked for providing and connecting the gas cylinders and reducers. A patent application titled "A Sensor for Detecting a Chemical Species and for Mitigating Drift" (NL2035557) with a priority date of 04-08-2023 has been submitted by Delft University of Technology.

References

[1] N. P. Brandon and Z. Kurban, "Clean energy and the hydrogen economy," *Phil. Trans. Roy. Soc. A, Math., Phys. Eng. Sci.*, vol. 375, no. 2098, 2017, Art. no. 20160400.

[2] "Hydrogen to the rescue," *Nature Mater.*, vol. 17, no. 565, 2018. [Online]. Available: https://www.nature.com/articles/s41563-018-0129-y

[3] J. O. Abe, A. P. I. Popoola, E. Ajenifuja, and O. M. Popoola, "Hydrogen energy, economy and storage: Review and recommendation," *Int. J. Hydrogen Energy*, vol. 44, no. 29, pp. 15072–15086, Jun. 2019.

[4] G. Glenk and S. Reichelstein, "Economics of converting renewable power to hydrogen," *Nature Energy*, vol. 4, no. 3, pp. 216–222, Feb. 2019.

[5] A. Bakenne, W. Nuttall, and N. Kazantzis, "Sankey-Diagram-based insights into the hydrogen economy of today," *Int. J. Hydrogen Energy*, vol. 41, no. 19, pp. 7744–7753, May 2016.

[6] A. El Kharbachi et al., "Metal hydrides and related materials. Energy carriers for novel hydrogen and electrochemical storage," *J. Phys. Chem. C*, vol. 124, no. 14, pp. 7599–7607, Apr. 2020.

[7] N. Warwick, P. Griffiths, J. Keeble, A. Archibald, J. Pyle, and K. Shine. (2022). *Atmospheric Implications of Increased Hydrogen Use*. [Online]. Available: https://assets.publishing.service.gov.uk/government/uploads/system/uploads/attachment_data/file/1067144/atmospheric-implications-of-increased-hydrogen-use.pdf

[8] T. Hübert, L. Boon-Brett, G. Black, and U. Banach, "Hydrogen sensors—A review," *Sens. Actuators B, Chem.*, vol. 157, no. 2, pp. 329–352, 2011.

[9] C. Wadell, S. Syrenova, and C. Langhammer, "Plasmonic hydrogen sensing with nanostructured metal hydrides," *ACS Nano*, vol. 8, no. 12, pp. 11925–11940, Dec. 2014.

[10] L. J. Bannenberg, C. Boelsma, K. Asano, H. Schreuders, and B. Dam, "Metal hydride based optical hydrogen sensors," *J. Phys. Soc. Jpn.*, vol. 89, no. 5, May 2020, Art. no. 051003.

[11] L. J. Bannenberg et al., "Metal (boro-) hydrides for high energy density storage and relevant emerging technologies," *Int. J. Hydrogen Energy*, vol. 45, no. 58, pp. 33687–33730, Nov. 2020.

[12] I. Darmadi, F. A. A. Nugroho, and C. Langhammer, "High-performance nanostructured palladium-based hydrogen sensors—Current limitations and strategies for their mitigation," *ACS Sensors*, vol. 5, no. 11, pp. 3306–3327, Nov. 2020.

[13] W.-T. Koo et al., "Chemiresistive hydrogen sensors: Fundamentals, recent advances, and challenges," *ACS Nano*, vol. 14, no. 11, pp. 14284–14322, Nov. 2020.

[14] K. Chen, D. Yuan, and Y. Zhao, "Review of optical hydrogen sensors based on metal hydrides: Recent developments and challenges," *Opt. Laser Technol.*, vol. 137, May 2021, Art. no. 106808.

[15] M. A. Butler, "Fiber optic sensor for hydrogen concentrations near the explosive limit," *J. Electrochem. Soc.*, vol. 138, no. 9, pp. 46–47, Sep. 1991.

[16] M. A. Butler and R. J. Buss, "Kinetics of the micromirror chemical sensor," *Sens. Actuators B, Chem.*, vol. 11, nos. 1–3, pp. 161–166, Mar. 1993.

[17] M. A. Butler, "Micromirror optical-fiber hydrogen sensor," *Sens. Actuators B, Chem.*, vol. 22, no. 2, pp. 155–163, Nov. 1994.

[18] C.-L. Tien, H.-W. Chen, W.-F. Liu, S.-S. Jyu, S.-W. Lin, and Y.-S. Lin, "Hydrogen sensor based on side-polished fiber Bragg gratings coated with thin palladium film," *Thin Solid Films*, vol. 516, no. 16, pp. 5360–5363, Jun. 2008.

[19] J. Dai, M. Yang, X. Yu, K. Cao, and J. Liao, "Greatly etched fiber Bragg grating hydrogen sensor with Pd/Ni composite film as sensing material," *Sens. Actuators B, Chem.*, vol. 174, pp. 253–257, Nov. 2012.

[20] J. Dai et al., "Enhanced sensitivity of fiber Bragg grating hydrogen sensor using flexible substrate," *Sens. Actuators B, Chem.*, vol. 196, pp. 604–609, Jun. 2014.

[21] B. Chadwick and M. Gal, "Enhanced optical detection of hydrogen using the excitation of surface plasmons in palladium," *Appl. Surf. Sci.*, vol. 68, no. 1, pp. 135–138, May 1993.

[22] C. Perrotton et al., "A reliable, sensitive and fast optical fiber hydrogen sensor based on surface plasmon resonance," *Opt. Exp.*, vol. 21, no. 1, pp. 382–390, Jan. 2013.

[23] F. A. A. Nugroho et al., "Metal-polymer hybrid nanomaterials for plasmonic ultrafast hydrogen detection," *Nature Mater.*, vol. 18, no. 5, pp. 489–495, May 2019.

[24] L. J. Bannenberg et al., "Optical hydrogen sensing beyond palladium: Hafnium and tantalum as effective sensing materials," *Sens. Actuators B, Chem.*, vol. 283, pp. 538–548, Mar. 2019.

[25] L. Bannenberg, H. Schreuders, and B. Dam, "Tantalum-palladium: Hysteresis-Free optical hydrogen sensor over 7 orders of magnitude in pressure with sub-second response," *Adv. Funct. Mater.*, vol. 31, no. 16, Apr. 2021, Art. no. 2010483.

[26] L. J. Bannenberg, H. Schreuders, N. van Beugen, C. Kinane, S. Hall, and B. Dam, "Tuning the properties of thin film TaRu for hydrogen sensing applications," *ACS Appl. Mater. Interfaces*, vol. 15, no. 6, pp. 8033–8045, 2023.

[27] L. J. Bannenberg, L. Blom, K. Sakaki, K. Asano, and H. Schreuders, "Completely elastic deformation of hydrogenated Ta thin films," *ACS Mater. Lett.*, vol. 5, no. 4, pp. 962–969, Apr. 2023.

Authorized licensed use limited to: TU Delft Library. Downloaded on January 18,2024 at 13:07:31 UTC from IEEE Xplore. Restrictions apply.

[28] M. Björck and G. Andersson, "GenX: An extensible X-ray reflectivity refinement program utilizing differential evolution," *J. Appl. Crystallogr.*, vol. 40, no. 6, pp. 1174–1178, Dec. 2007.
[29] A. Glavic and M. Björck, "GenX 3: The latest generation of an established tool," *J. Appl. Crystallogr.*, vol. 55, no. 4, pp. 1063–1071, Aug. 2022.
[30] L. J. Bannenberg, B. Boshuizen, F. A. Ardy Nugroho, and H. Schreuders, "Hydrogenation kinetics of metal hydride catalytic layers," *ACS Appl. Mater. Interfaces*, vol. 13, no. 44, pp. 52530–52541, Nov. 2021.
[31] D. J. Verhoeff, "Towards a practical hydrogen sensor; optical response analysis on new geometries for $Ta_{0.88}Pd_{0.12}$ based metal-hydride hydrogen sensors, and characterisation of structure at low temperatures," M.S. thesis, Delft Univ. Technol., Delft, The Netherlands, 2023.
[32] Y. Fukai, *The Metal-Hydrogen System: Basic Bulk Properties*, vol. 21. Berlin, Germany: Springer, 2006.
[33] W. M. Mueller, J. P. Blackledge, and G. G. Libowitz, *Metal Hydrides*. Amsterdam, The Netherlands: Elsevier, 2013.

Lars J. Bannenberg received the M.Sc. degree in financial economics from Erasmus University Rotterdam, Rotterdam, The Netherlands, in 2015, and the M.Sc. degree in applied physics and the Ph.D. degree in skyrmions and cubic chiral magnetism from the Delft University of Technology, Delft, The Netherland, in 2019.

Since his master's thesis, he has been studying (thin-film) metal hydrides for a variety of applications: first, as hydrogen storage materials and currently for optical hydrogen-sensing applications. For example, creating an all-optical hydrogen sensor based on a tantalum alloy that can detect hydrogen over seven orders of magnitude in hydrogen concentration with subsecond response times. He is an Instrument Scientist of neutron reflectometer at the TU Delft Reactor Institute, Delft, and studies batteries and other energy materials. He is currently an Assistant Professor with the Faculty of Applied Sciences, Delft University of Technology. His research interests include understanding the structure of materials and relating it to their functional properties. To do so, he applies a wide variety of experimental techniques with a focus on X-ray and neutron scattering such as diffraction, spectroscopy, and reflectometry.

Authorized licensed use limited to: TU Delft Library. Downloaded on January 18,2024 at 13:07:31 UTC from IEEE Xplore. Restrictions apply.